EUROPHYSICS LETTERS 15 March 2006

Europhys. Lett., **73** (6), pp. 920–926 (2006)
DOI: 10.1209/epl/i2006-10002-4

Origin of the inner ring in photoluminescence patterns of quantum well excitons

A. L. Ivanov[1], L. E. Smallwood[1], A. T. Hammack[2], Sen Yang[2], L. V. Butov[2] and A. C. Gossard[3]

[1] *Department of Physics and Astronomy, Cardiff University - Cardiff CF24 3YB, UK*
[2] *Department of Physics, University of California at San Diego La Jolla, CA 92093-0319, USA*
[3] *Materials Department, University of California at Santa Barbara Santa Barbara, CA 93106-5050, USA*

received 18 January 2006; accepted in final form 30 January 2006
published online 15 February 2006

PACS. 71.35.-y – Excitons and related phenomena.
PACS. 73.63.Hs – Electronic transport in nanoscale materials and structures: Quantum wells.
PACS. 78.67.De – Optical properties of low-dimensional, mesoscopic, and nanoscale materials and structures: Quantum wells.

Abstract. – In order to explain and model the *inner ring* in photoluminescence (PL) patterns of indirect excitons in GaAs/AlGaAs quantum wells (QWs), we develop a microscopic approach formulated in terms of coupled nonlinear equations for the diffusion, thermalization and optical decay of the particles. The origin of the inner ring is unambiguously identified: it is due to cooling of indirect excitons in their propagation from the excitation spot.

More than two decades ago, long-distance diffusion and drift transport of charge-neutral excitons with a long lifetime was optically visualized in bulk Si and Cu_2O [1,2]. In these earlier works, strain gradient potential traps were used to induce the drift motion. Due to the low particle concentrations, the transport was described in terms of a classical picture, with no quantum-statistical corrections, and the diffusion coefficient was attributed to exciton-phonon scattering. In-plane propagation of long-lived indirect excitons in coupled QWs over large distances has also been reported [3–7]: in this case one has a unique possibility to optically map the quasi–two-dimensional motion of composite bosons. Furthermore, the density n_{2d} of indirect excitons can be large enough to ensure nonclassical population of the ground-energy state, $N_{E=0} = e^{T_0/T} - 1 \geq 1$, where $T_0 = (\pi\hbar^2 n_{2d})/(2k_B M_x)$ and T are the degeneracy temperature and exciton temperature, respectively, and M_x is the exciton in-plane translational mass (for a recent review of cold exciton gases in coupled QWs see ref. [8]).

One of the most striking features of photoluminescence associated with indirect excitons is the appearance of two *PL rings* [6]. While the second, external ring has already been explained in terms of in-plane spatially separated electrons and holes [9,10], the origin of the first, inner ring, which arises purely due to the transport of indirect excitons, remained unclear. The underlying physical picture we propose to explain this ring is that in the optically-pumped area the exciton temperature T is much larger than the lattice temperature T_b. As a result, the optical decay of excitons is suppressed, but while they diffuse out they cool down and eventually become optically-active, giving rise to a local increase of the PL signal.

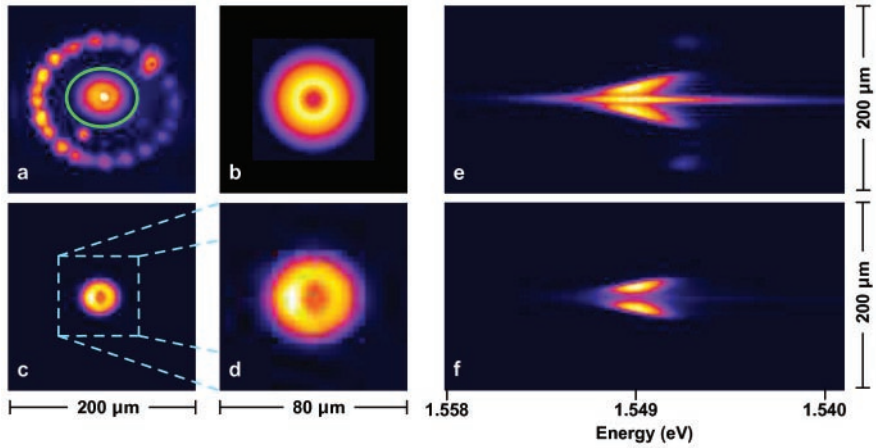

Fig. 1 – (Color online) Experimental (a), (c)-(f) and calculated (b) patterns of the PL signal from indirect excitons. In (a), the PL intensity in the area within the green circle is reduced by a constant factor for better visualization. A bright spot in the middle of the inner ring in (a) is due to residual bulk emission. (e) and (f) Image of the PL signal in E-x coordinates. The external PL ring is also seen for high excitations, both in (a) x-y and (e) E-x coordinates. For (a) and (e) the excitation power is $P_{\rm ex} = 250\,\mu$W and for (b)-(d) and (f) $P_{\rm ex} = 75\,\mu$W and $T_{\rm b} = 1.5\,$K.

In this letter we develop a microscopic theory for the long-range transport, thermalization and optical decay of QW excitons, model the inner PL ring, show an effective screening of QW disorder for $n_{\rm 2d} \geq 10^{10}\,{\rm cm}^{-2}$, and analyze the quantum-statistical corrections. By numerically fitting the PL spectra we clarify the main scattering channels which contribute to the diffusion of indirect excitons, and evaluate the diffusion coefficient and amplitude of the QW disorder potential. In the proposed model, the exciton temperature T is affected by heating due to the optical excitation, heating due to the LA-phonon assisted conversion of the mean-field energy into the internal energy and recombination heating or cooling due to the optical decay of low-energy excitons. The mean-field energy of indirect excitons also gives rise to a potential energy gradient and, therefore, to the in-plane drift motion.

In the experiments, the PL pattern is imaged by a nitrogen-cooled CCD camera with the spectral selection by an interference filter adjusted to the indirect exciton energy. Fine adjustment of the filtering energy is done by rotating two interference filters relative to the optical axis. As a result, we are able to remove the low-energy bulk emission that otherwise dominates the spectrum near the excitation spot [6] and observe a two-dimensional spatial image of the inner ring (see figs. 1a, c and d). Note that the inner PL ring can be missed if the bulk emission is not removed from the PL signal. In figs. 1e and f we plot the measured exciton PL in the *energy-coordinate* plane. The exciton energy $E_{\rm PL}$ decreases with increasing distance from the excitation spot, as detailed below. This results in an arrow-shaped profile of the exciton PL images in the E-x coordinates. The external ring is also seen at high excitations, both in x-y (fig. 1a) and E-x (fig. 1e) coordinates. The excitation is done by a HeNe laser at 633 nm (the laser spot is a Gaussian with FWHM $\simeq 6\,\mu$m, the excitation power $P_{\rm ex} = 1$–$400\,\mu$W). The coupled QW structure with two 8 nm GaAs QWs separated by a 4 nm $Al_{0.33}Ga_{0.67}As$ barrier is grown by molecular beam epitaxy.

The PL from indirect excitons, which are created by conversion of resonantly excited light-hole direct excitons, is also studied by using a Ti:Sapphire laser. For this subbarrier excitation,

no excess free carriers are photogenerated and the external ring is absent [9,10]. However, as shown in fig. 2d, the inner ring is clearly seen. This proves the excitonic origin of the ring. In further analysis we will consider excitation at 633 nm, due to a much larger ratio between the excitonic PL signal and bulk emission background.

Our approach to the transport, relaxation and PL dynamics of indirect excitons is formulated in terms of three coupled nonlinear equations: a quantum diffusion equation for n_{2d}, a thermalization equation for T, and an equation for the optical lifetime $\tau_{opt} = 1/\Gamma_{opt}$. The quantum-statistical corrections, which enhance the nonlinear effects, are included in the description. The underlying physical picture we use refers to the relaxation thermodynamics [11] and assumes a hierarchy of interactions, *i.e.* that the QW exciton – QW exciton scattering is more efficient than the interaction of QW excitons with bulk LA-phonons. This means that thermalization of QW excitons occurs through the quasi-equilibrium thermodynamic states, which are completely characterized by T and $T_0 \propto n_{2d}$. The relaxation thermodynamics deals with concentrations $10^9\,\mathrm{cm}^{-2} \le n_{2d} < 10^{11}\,\mathrm{cm}^{-2}$ [11] which are relevant to our experiments.

The nonlinear diffusion equation [12] is given by

$$\frac{\partial n_{2d}}{\partial t} = \nabla\Big[D_x^{(2d)}\nabla n_{2d} \;+\; \mu_x^{(2d)} n_{2d}\nabla\left(u_0 n_{2d} + U_{QW}\right)\Big] - \Gamma_{opt} n_{2d} + \Lambda\,, \tag{1}$$

where Γ_{opt}, $D_x^{(2d)}$, $\mu_x^{(2d)}$ and Λ are the radiative decay rate, diffusion coefficient, mobility and generation rate of QW excitons, respectively, $U_{QW} = U_{rand}(\boldsymbol{r}_\parallel)$ is a random potential due to the QW thickness and alloy fluctuations, and the operator ∇ is defined in terms of the in-plane coordinate vector $\boldsymbol{r}_\parallel$. The *generalized Einstein relationship* [12], $\mu_x^{(2d)} = D_x^{(2d)}[(e^{T_0/T}-1)/(k_B T_0)]$, which yields the classical limit $\mu_x^{(2d)} = D_x^{(2d)}/(k_B T)$ for $T \gg T_0$, strongly enhances the nonlinearity of the diffusion equation (1) for $T \le T_0$. In the latter case, eq. (1) becomes T_0-dependent and, therefore, explicitly includes the quantum statistical corrections through $T_0 \propto \hbar^2$. The positive mean-field energy $u_0 n_{2d}$ on the right-hand side of eq. (1) is due to the well-defined dipole-dipole repulsive interaction of indirect excitons [13,14]. Here $u_0 = 4\pi(e^2/\varepsilon_b)d_z$, ε_b is the background dielectric constant, and d_z is the separation between electron and hole layers. The mean-field energy gives rise to the in-plane drift motion with the velocity $\boldsymbol{v}_{drift} = -\mu_x^{(2d)} u_0 \nabla n_{2d}$. As a result, an effective screening of the disorder potential U_{rand} by dipole-dipole interacting indirect excitons builds up with increasing n_{2d} [12,15]: the excitons tend to accumulate near the minima of $U_{rand}(\boldsymbol{r}_\parallel)$ (local increase of $u_0 n_{2d}(\boldsymbol{r}_\parallel)$) and avoid the maxima of $U_{rand}(\boldsymbol{r}_\parallel)$ (local decrease of $u_0 n_{2d}(\boldsymbol{r}_\parallel)$). As we show below, in our high-quality structures $U^{(0)} = 2\langle|U_{rand}(\boldsymbol{r}_\parallel)|\rangle \simeq 0.9\,\mathrm{meV}$ and the mean-free energy $u_0 n_{2d}^{(0)} \simeq 1.6\,\mathrm{meV}$ for $n_{2d}^{(0)} = 10^{10}\,\mathrm{cm}^{-2}$, so that at low exciton temperatures $T \sim 1\,\mathrm{K}$ the QW disorder is strongly screened and practically removed for $n_{2d} \ge n_{2d}^{(0)}$.

The temperature dynamics of excitons is given by

$$\frac{\partial}{\partial t}T \;=\; \left(\frac{\partial T}{\partial t}\right)_{n_{2d}} + \;\frac{S_{pump} + S_{opt} + S_d}{2k_B T I_1 - k_B T_0 I_2}\,, \tag{2}$$

$$\left(\frac{\partial T}{\partial t}\right)_{n_{2d}} = -\frac{2\pi}{\tau_{sc}}\left(\frac{T^2}{T_0}\right)\left(1-e^{-T_0/T}\right)\int_1^\infty \mathrm{d}\varepsilon\;\varepsilon\sqrt{\frac{\varepsilon}{\varepsilon-1}}\;\times$$
$$\times\,\frac{|F_z(a\sqrt{\varepsilon(\varepsilon-1)}|^2}{(e^{\varepsilon E_0/k_B T_b}-1)}\;\frac{e^{\varepsilon E_0/k_B T_b} - e^{\varepsilon E_0/k_B T}}{(e^{\varepsilon E_0/k_B T} + e^{-T_0/T} - 1)}\,, \tag{3}$$

where $I_1 = (1-e^{-T_0/T})\int_0^\infty \mathrm{d}z[z/(e^z + e^{-T_0/T} - 1)]$, $I_2 = e^{-T_0/T}\int_0^\infty \mathrm{d}z[(ze^z)/(e^z + e^{-T_0/T} - 1)^2]$. Equation (3) describes the LA-phonon assisted thermalization of indirect excitons: $\tau_{sc} =$

$(\pi^2\hbar^4\rho)/(D_{\rm dp}^2 M_{\rm x}^3 v_{\rm s})$ is the characteristic scattering time, $E_0 = 2M_{\rm x}v_{\rm s}^2$, $v_{\rm s}$ is the longitudinal sound velocity, ρ is the crystal mass density, and $D_{\rm dp}$ is the deformation potential of exciton – LA-phonon interaction. The form-factor $F_z(\chi) = [\sin(\chi)/\chi][e^{i\chi}/(1-\chi^2/\pi^2)]$ refers to a QW confinement potential and characterizes a spectral band of bulk LA-phonons which interact with indirect excitons, $a = (d_{\rm QW}M_{\rm x}v_{\rm s})/\hbar$, and $d_{\rm QW}$ is the QW thickness. For $1.5\,{\rm K} \leq T \leq 6.5\,{\rm K}$ and $n_{\rm 2d} = 10^{10}\,{\rm cm}^{-2}$, relevant to our experiments, eq. (3) yields a thermalization time $0.15\,{\rm ns} \geq \tau_{\rm th} \geq 0.03\,{\rm ns}$. The strong increase of $\tau_{\rm th}$ with decreasing T is due to classical slowing-down of the relaxation kinetics, which occurs at $k_{\rm B}T \sim E_0$ (excitons with energies $E \leq E_0/4$ cannot emit LA-phonons) [11, 16, 17].

Heating of indirect excitons by the laser pulse is given by the term $S_{\rm pump} = (E_{\rm inc} - k_{\rm B}TI_2)\Lambda_{T_0} > 0$ on the right-hand side of eq. (2). Here, $\Lambda_{T_0} = [(\pi\hbar^2)/(2k_{\rm B}M_{\rm x})]\Lambda(t, \boldsymbol{r}_\parallel)$. The generation of indirect excitons is a secondary process, mainly due to quantum tunnelling of photoexcited direct excitons to the energetically more favorable states of indirect excitons. The excess energy $E_{\rm inc}$ of a created (incoming) indirect exciton is large: it exceeds the energy splitting between the direct and indirect excitons, which is about 20 meV. For the highest generation rates used in the experiments, the exciton temperature $T^{\rm max} \simeq 6.4\,{\rm K}$ at the laser spot center is much larger than $T_{\rm b} \simeq 1.5\,{\rm K}$.

Recombination heating or cooling of QW excitons [17] is given by the term $S_{\rm opt} = [k_{\rm B}TI_2\Gamma_{\rm opt} - E_\gamma\Gamma_{\rm opt}^{\rm E}]T_0$ on the right-hand side of eq. (2), where

$$\Gamma_{\rm opt} = \frac{1}{2\tau_{\rm R}}\left(\frac{E_\gamma}{k_{\rm B}T_0}\right)\int_0^1 \frac{1+z^2}{Be^{-z^2E_\gamma/k_{\rm B}T}-1}\,{\rm d}z \tag{4}$$

and $\Gamma_{\rm opt}^{\rm E} = [E_\gamma/(2\tau_{\rm R}k_{\rm B}T_0)]\int_0^1[(1-z^4)/(Be^{-z^2E_\gamma/k_{\rm B}T}-1)]\,{\rm d}z$ are the optical decay rates for the concentration and energy density of indirect excitons, respectively, $\tau_{\rm R}$ is the intrinsic radiative lifetime of indirect excitons, $E_\gamma = p_0^2/(2M_{\rm x})$, $B = (e^{E_\gamma/k_{\rm B}T})/(1-e^{-T_0/T})$, and $p_0 = (E_{\rm x}\sqrt{\varepsilon_{\rm b}})/c$ ($E_{\rm x}$ is the total energy of a ground-state indirect exciton). In contrast with the evaporative cooling schemes used in atomic optics to remove high-energy atoms from magnetic traps [18, 19], the optical evaporation of QW excitons is an inherent process, which deals with the lowest-energy particles, $0 \leq E \leq E_\gamma$, from the radiative zone. Both signs of $S_{\rm opt}$ can be realized: $S_{\rm opt} > 0$ ($S_{\rm opt} < 0$), *i.e.* recombination heating (cooling) of indirect excitons for $k_{\rm B}T \geq E_\gamma$ and $k_{\rm B}T_0$ ($k_{\rm B}T \ll E_\gamma$ and $k_{\rm B}T_0$). In our case recombination heating occurs: far away from the excitation spot T exceeds $T_{\rm b}$ by about 3 mK, *i.e.* due to relatively high $T_{\rm b}$, the effect is small. Note that an effective recombination cooling of particles takes place for $T_{\rm b} \leq 0.1\,{\rm K}$: the effect is strong and reduces $\tau_{\rm th}$ by $\geq 20\%$.

Heating of excitons by in-plane drift is given by $S_{\rm d} = -T_0u_0(\boldsymbol{v}_{\rm tot}\cdot\nabla n_{\rm 2d})$ on the right-hand side of eq. (2), where $\boldsymbol{v}_{\rm tot} = \boldsymbol{v}_{\rm diff} + \boldsymbol{v}_{\rm drift}$ and $\boldsymbol{v}_{\rm diff} = -(D_{\rm x}^{\rm (2d)}/n_{\rm 2d})\nabla n_{\rm 2d}$. This heating mechanism is due to conversion of the mean-field energy into the internal one. The effect is particularly well defined for $k_{\rm B}T \gg E_0$ ($E_0/k_B \simeq 0.4\,{\rm K}$), when the momentum relaxation time is much less than $\tau_{\rm th}$.

In our model, the diffusion coefficient $D_{\rm x}^{\rm (2d)} = (D_{\rm x-x}^{\rm (2d)}D_{\rm x-imp}^{\rm (2d)})/(D_{\rm x-x}^{\rm (2d)} + D_{\rm x-imp}^{\rm (2d)})$ has two contributions: diffusion due to scattering by imperfections (QW impurities and bulk LA-phonons), with $D_{\rm x-imp}^{\rm (2d)} = D_{\rm x-imp}^{\rm (2d)}(T_{\rm b})$, and self-diffusion due to exciton-exciton scattering. The latter channel is important for $n_{\rm 2d} \geq 10^{10}\,{\rm cm}^{-2}$ and $D_{\rm x-x}^{\rm (2d)}$ is approximated by $D_{\rm x-x}^{\rm (2d)} = C_{\rm x-x}(T/T_0)$ [12]. For $r_\parallel$ far away from the excitation spot, the asymptotic solution of eqs. (1)-(4) yields $I_{\rm PL} \propto \exp[-(\Gamma_{\rm opt}/D_{\rm x-imp}^{\rm (2d)})^{1/2}r_\parallel]$. In contrast, the experimental data show a much steeper decay of the PL signal and its *spatial pinning* at a critical radius $r_\parallel^{\rm cr} = r_\parallel^{\rm cr}(P_{\rm ex})$ (*e.g.*, $r_\parallel^{\rm cr} \simeq 40\,\mu{\rm m}$ for $P_{\rm ex} = 402\,\mu{\rm W}$, see fig. 2a). We attribute such a behaviour to the

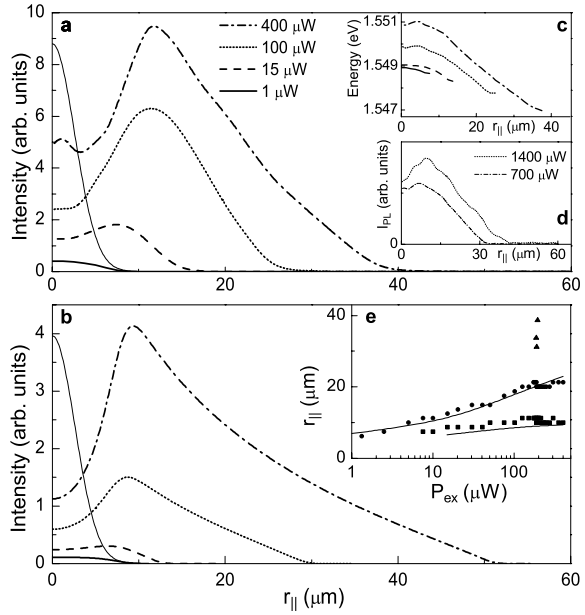

Fig. 2 – The PL intensity of indirect excitons $I_{\rm PL}$, (a) measured and (b) calculated with eqs. (1)-(4), against radius $r_\parallel$ for four optical excitation powers $P_{\rm ex}$. The Gaussian profile of the optical excitation is shown by the thin solid lines. The cryostat temperature $T_{\rm b} = 1.5\,{\rm K}$. In numerical evaluations the following parameters are used: $D_{\rm dp} = 9.6\,{\rm eV}$, $\tau_{\rm R} = 13\,{\rm ns}$, $E_{\rm inc}/k_{\rm B} = 200\,{\rm K}$, $M_{\rm x} = 0.215\,m_0$, $d_{\rm QW} = 8\,{\rm nm}$, and $d_z = 11.5\,{\rm nm}$. The best fitting parameters are $U_0 = 0.9\,{\rm meV}$, $D^{(2d)}_{\rm x-imp} = 60\,{\rm cm}^2/{\rm s}$ and $C_{\rm x-x} = 15\,{\rm cm}^2/{\rm s}$. (d) $I_{\rm PL} = I_{\rm PL}(r_\parallel)$ of indirect excitons measured at subbarrier excitation (780 nm) for $P_{\rm ex} = 0.7\,{\rm mW}$ and $1.4\,{\rm mW}$. Bulk emission is subtracted from the total PL signal in (a) and (d). The energy position of the PL line, $E_{\rm PL} = E_{\rm PL}(r_\parallel)$ for the data shown in (a) is plotted in (c). (e) The measured (square points) and calculated (solid line) inner ring radius $r^{\rm rg}_\parallel$ *vs.* $P_{\rm ex}$ (the triangular points refer to the external PL ring), and the measured (circle points) and calculated (solid line) HWHM spatial extension of the PL signal against $r_\parallel$.

$n_{2\rm d}$-dependent screening of long-range-correlated QW disorder by dipole-dipole interacting indirect excitons. The narrowing effect is illustrated in fig. 3a for a particular realization of the disorder potential $U_{\rm rand}(r_\parallel)$. In order to include the long-range-correlated disorder we use a *thermionic model*, which operates with $n_{2\rm d}$- and T-dependent diffusion coefficient $\tilde{D}^{(2{\rm d})}_{\rm x} = D^{(2{\rm d})}_{\rm x} \exp[-U^{(0)}/(k_{\rm B}T + u_0 n_{2\rm d})]$ [12].

In order to model the experimental results within the developed microscopic picture, we solve eqs. (1)-(4) numerically for a stationary, cylindrically-symmetric optical excitation profile, so that the generation rate $\Lambda(\boldsymbol{r}_\parallel, t) \equiv \Lambda(r_\parallel) \propto P_{\rm ex} \exp[-r^2_\parallel/\sigma^2]$. The best fit for the experimental data plotted in fig. 2a (see also fig. 1b) yields $U_0 = 0.9\,{\rm meV}$, $D^{(2{\rm d})}_{\rm x-imp} = 60\,{\rm cm}^2/{\rm s}$ and $C_{\rm x-x} = 15\,{\rm cm}^2/{\rm s}$. The calculated spatial profile of the PL signal, $I_{\rm PL} = I_{\rm PL}(r_\parallel)$, is shown in fig. 2b for various pump powers $P_{\rm ex}$. While the density profile $n_{2\rm d} = n_{2\rm d}(r_\parallel)$ always has a bell-like shape (see fig. 3b and fig. 2c), with increasing $P_{\rm ex}$ the inner PL ring develops in the $I_{\rm PL}$-profile. This is in complete agreement with the observations. The inner ring has a nearly classical origin and arises due to heating of indirect excitons by the optical excitation ($S_{\rm pump}$ term in eq. (2)): with increasing $r_\parallel$ the exciton temperature T rapidly decreases towards $T_{\rm b}$

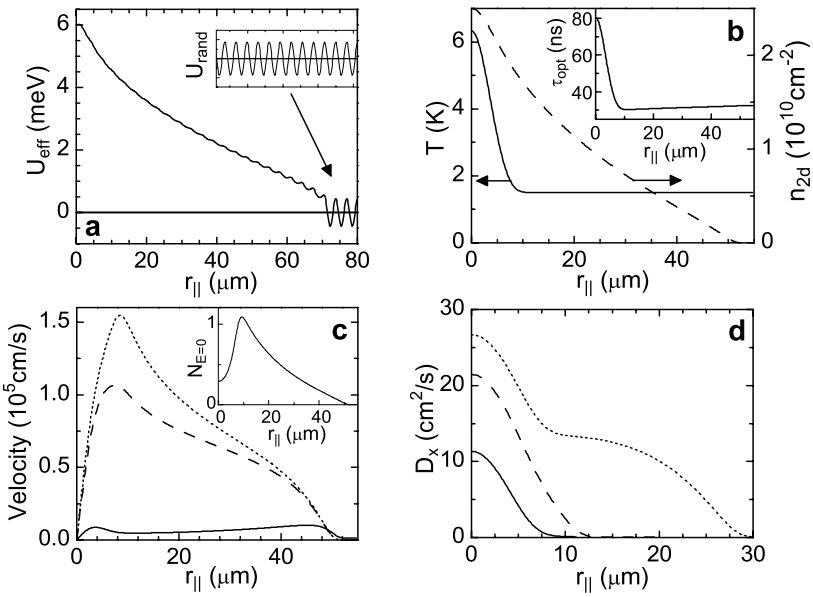

Fig. 3 – (a) The narrowing effect: screening of the long-range-correlated disorder potential $U_{\rm rand}(\boldsymbol{r}_\parallel)$ by dipole-dipole interacting indirect excitons. The QW effective potential $U_{\rm eff}(r_\parallel) = U_{\rm rand}(r_\parallel) + u_0 n_{\rm 2d}(r_\parallel)$ calculated with eqs. (1)-(4) for harmonic $U_{\rm rand}(r_\parallel)$ with $U_0/2 = 0.45\,$meV (see the inset). (b) $T = T(r_\parallel)$ (solid line) and $n_{\rm 2d} = n_{\rm 2d}(r_\parallel)$ (dashed line). Inset: $\tau_{\rm opt} = \tau_{\rm opt}(r_\parallel)$. (c) Diffusion velocity $v_{\rm diff} = v_{\rm diff}(r_\parallel)$ (solid line) and drift velocity $v_{\rm drift} = v_{\rm drift}(r_\parallel)$ without (dashed line) and with (dotted line) quantum-statistical corrections. Inset: $N_{E=0} = N_{E=0}(r_\parallel)$. Plots (a)-(c) refer to the maximum excitation, $n_{\rm 2d}^{\rm max} = 2.5\times10^{10}\,{\rm cm}^{-2}$ (see the dash-dotted lines in fig. 2). (d) Diffusion coefficient $D_{\rm x} = \tilde{D}_{\rm x}^{\rm (2d)}(r_\parallel)$ for $n_{\rm 2d}^{\rm max} = 0.16\times10^{10}\,{\rm cm}^{-2}$ (solid line), $0.44\times10^{10}\,{\rm cm}^{-2}$ (dashed line) and $1.27\times10^{10}\,{\rm cm}^{-2}$ (dotted line). These values of $n_{\rm 2d}^{\rm max}$ correspond to the PL signal shown in fig. 2.

(see fig. 3b); as a result, the optical lifetime $\tau_{\rm opt} = 1/\Gamma_{\rm opt}$ decreases too (see the inset of fig. 3b), giving rise to a local increase of $I_{\rm PL}(r_\parallel)$ at $r_\parallel = r_\parallel^{\rm rg}$. Thus the inner ring is a spatial counterpart of the PL-jump observed in the time-resolved experiments [20]. Our numerical simulations also reproduce the observed increase of $r_\parallel^{\rm rg}$ and the spatial extension of the PL area (HWHM of the signal) with increasing $P_{\rm ex}$ (see fig. 2e).

The finding of the fitting parameters, which refer to the total diffusion coefficient $\tilde{D}_{\rm x}^{\rm (2d)}$, is *complex*, *i.e.* we fit all the curves plotted in figs. 2a and c ($I_{\rm PL} = I_{\rm PL}(r_\parallel)$ and $E_{\rm PL} = E_{\rm PL}(r_\parallel)$ for various $P_{\rm ex}$) by using the same values of U_0, $D_{\rm x-imp}^{\rm (2d)}$ and $C_{\rm x-x}$. The blue shift $\delta_{\rm PL} \geq 0$ of the PL energy $E_{\rm PL}$ is due to the mean-field interaction energy of indirect excitons, $\delta_{\rm PL} = E_{\rm PL} - E_{\rm x} = u_0 n_{\rm 2d}$ (see figs. 1e-f and 2c). Thus we use the measured $\delta_{\rm PL}$ to estimate $n_{\rm 2d}^{\rm max}(r_\parallel = 0)$, and therefore the generation rate $\Lambda(r_\parallel = 0)$, necessary for numerical modelling with eqs. (1)-(4). The amplitude of the disorder potential U_0 determines the steepness of $I_{\rm PL}(r_\parallel > r_\parallel^{\rm rg})$ and dependence $r_\parallel^{\rm cr} = r_\parallel^{\rm cr}(P_{\rm ex})$ of the PL pinning radius. In turn, $D_{\rm x-imp}^{(2d)}$ and $C_{\rm x-x}$ determine the ring contrast and $r_\parallel^{\rm rg} = r_\parallel^{\rm rg}(P_{\rm ex})$ dependence. The total diffusion coefficient $\tilde{D}_{\rm x}^{\rm (2d)} = \tilde{D}_{\rm x}^{\rm (2d)}(r_\parallel)$ is plotted in fig. 3d. Outside the excitation spot, for $r_\parallel \simeq r_\parallel^{\rm cr}$, we approximate $\tilde{D}_{\rm x}^{\rm (2d)} \simeq D_{\rm x-imp}^{\rm (2d)} \exp[-U^{(0)}/(k_{\rm B}T_{\rm b})]$. With our fitting parameters one estimates

$\tilde{D}_{\mathrm{x}}^{(2\mathrm{d})}(T_{\mathrm{b}}=1.8\,\mathrm{K}, r_{\parallel}\simeq r_{\parallel}^{\mathrm{cr}}) \simeq 0.18\,\mathrm{cm}^2/\mathrm{s}$. The value is consistent with that reported in ref. [7].

In fig. 3c we show that for the small excitation spot ($\sigma \simeq 3\,\mu\mathrm{m}$) used in the experiments, the drift velocity v_{drift}, due to the gradient of the mean-field interaction energy $u_0 n_{2\mathrm{d}}(r_{\parallel})$, is much larger than the diffusion velocity v_{diff}. The total velocity has a maximum value $v_{\mathrm{tot}}^{\mathrm{max}}(r_{\parallel} \simeq r_{\parallel}^{\mathrm{rg}}) \simeq 1.5 \times 10^5\,\mathrm{cm/s}$ for $n_{2\mathrm{d}}^{\mathrm{max}}(r_{\parallel} = 0) \simeq 2.5 \times 10^{10}\,\mathrm{cm}^{-2}$ (see fig. 3c). Note that in our case the mean-field energy gradient $u_0|\nabla n_{2\mathrm{d}}(r_{\parallel} \simeq r_{\parallel}^{\mathrm{rg}})| \simeq 1.6\,\mathrm{eV/cm}$ exceeds the maximum strain-induced gradient $|\nabla U| \simeq 0.4\,\mathrm{eV/cm}$ used in the experiments [1, 2].

Finally, we emphasize that in our experiments, which deal with the cryostat temperature $T_{\mathrm{b}} = 1.5\,\mathrm{K}$, nonclassical occupation numbers of modest values, $N_{E=0}^{\mathrm{max}}(r_{\parallel} \simeq r_{\parallel}^{\mathrm{rg}}) \simeq 1$, build up at the position of the inner ring (see the inset of fig. 3c). As illustrated in fig. 3c, in this case the quantum statistical corrections, *e.g.*, to v_{diff} and to the Einstein relationship, are about 35% and therefore cannot be neglected. Nonclassical statistics occurs at the position of the inner ring, where the exciton gas is already cold but still dense. Furthermore, for $T_{\mathrm{b}} \sim 0.1\,\mathrm{K}$ (not yet realized in an optical imaging experiment) numerical modelling with eqs. (1)-(4) gives well-developed Bose-Einstein statistics with $N_{E=0}^{\mathrm{max}}(r_{\parallel} \simeq r_{\parallel}^{\mathrm{rg}}) \gg 1$.

* * *

We appreciate valuable discussions with L. V. Keldysh, L. S. Levitov, L. Mouchliadis and B. D. Simons. Support of this work by EU RTN Project HPRN-2002-00298 and ARO Project W911NF-05-1-0527 is gratefully acknowledged.

REFERENCES

[1] Tamor M. A. and Wolfe J. P., *Phys. Rev. Lett.*, **44** (1980) 1703.
[2] Trauernicht D. P., Wolfe J. P. and Mysyrowicz A., *Phys. Rev. Lett.*, **52** (1984) 855.
[3] Hagn M., Zrenner A., Böhm G. and Weimann G., *Appl. Phys. Lett.*, **67** (1995) 232.
[4] Negoita V., Snoke D. W. and Eberl K., *Phys. Rev. B*, **60** (1999) 2661.
[5] Larionov A. V., Timofeev V. B., Hvam J. and Soerensen K., *JETP*, **90** (2000) 1093.
[6] Butov L. V., Gossard A. C. and Chemla D. S., *Nature*, **418** (2002) 751.
[7] Vörös Z., Balili R., Snoke D. W., Pfeiffer L. and West K., *Phys. Rev. Lett.*, **94** (2005) 226401.
[8] Butov L. V., *J. Phys. Condens. Matter*, **16** (2004) R1577.
[9] Butov L. V., Levitov L. S., Mintsev A. V., Simons B. D., Gossard A. C. and Chemla D. S., *Phys. Rev. Lett.*, **92** (2004) 117404.
[10] Rapaport R., Chen G., Snoke D., Simon S. H., Pfeiffer L., West K., Liu Y. and Denev S., *Phys. Rev. Lett.*, **92** (2004) 117405.
[11] Ivanov A. L., Littlewood P. B. and Haug H., *Phys. Rev. B*, **59** (1999) 5032.
[12] Ivanov A. L., *Europhys. Lett.*, **59** (2002) 586.
[13] Butov L. V., Zrenner A., Abstreiter G., Böhm G. and Weimann G., *Phys. Rev. Lett.*, **73** (1994) 304.
[14] Zhu X., Littlewood P. B., Hybertsen M. and Rice T. M., *Phys. Rev. Lett.*, **74** (1995) 1633.
[15] Zimmermann R., *Solid State Commun.*, **134** (2005) 43.
[16] Soroko A. V. and Ivanov A. L., *Phys. Rev. B*, **65** (2002) 165310.
[17] Ivanov A. L., *J. Phys. Condens. Matter*, **16** (2004) S3629.
[18] Cornell E. A. and Wieman C. E., *Rev. Mod. Phys.*, **74** (2002) 875.
[19] Ketterle W., *Rev. Mod. Phys.*, **74** (2002) 1131.
[20] Butov L. V., Ivanov A. L., Imamoglu A., Littlewood P. B., Shashkin A. A., Dolgopolov V. T., Campman K. L. and Gossard A. C., *Phys. Rev. Lett.*, **86** (2001) 5608.